Dynamic Properties on NMR Spectroscopy of Non-Aqueous Electrolyte Solution Coexisting with Fumed Silica Dispersion

Takemoto, Marie
Maki, Hideshi
Mizuhata, Minoru

(Citation)
ECS Transactions,75(19):1-9

(Issue Date)
2017

(Resource Type)
journal article

(Version)
Version of Record

ECS Transactions, 75 (19) 1-9 (2017)
10.1149/07519.0001ecst ©The Electrochemical Society

Dynamic Properties on NMR Spectroscopy of Non-Aqueous Electrolyte Solution Coexisting with Fumed Silica Dispersion

Marie Takemoto[1], Hideshi Maki[1,2], Minoru Mizuhata[1]

[1]Department of Chemical Science and Engineering, Graduate School of Engineering, Kobe University, 1-1 Rokkodai-cho, Nada, Kobe 657-8501, Japan

[2]Center for Environmental Management, Kobe University, 1-1 Rokkodai-cho, Nada, Kobe 657-8501, Japan

In this study, the non-aqueous $LiClO_4$ solution mixed with fumed silica as model system of LIBs was applied, and the dynamic properties and influences which solvent molecules received from solid phase or Li^+ ion in using the NMR spectroscopy and the relaxation time (T_1, T_2) measurements were evaluated. The NMR signal of ^1H in PC molecules is influenced by coexisting solid phase in $LiClO_4$-PC solution /oxide powder. The dynamic property of the PC molecules drastically decreased in comparison with the system of the liquid only system. In IR spectra of PC/Alumina systems, the vibration in higher wavenumber range are predominantly observed due to indirect electron-donation from solid surface. The signal intensity depends on influenced liquid content from solid phase. Especially, the $LiClO_4$-PC solution /alumina systems, the intensity is abruptly decreased due to widely spread influences of solid phases. Moreover, the influence from the solid phase to the PC molecules is much smaller than the water molecules from the 1H spin-spin relaxation time (T_2). As for the electrolyte concentration dependence, PC system was more remarkable than the water solution system, namely the network structure of the whole PC solvent is greatly affected by the addition of the Li^+ ion, and it is thought that relaxation time largely decreased.

Introduction

In recent years, lithium ion battery (LIBs) is indispensable to various electrochemical devices in practical use such as a cell phone, electric vehicle due to its high energy density, high voltage. However, with the diversification of the use, batteries which have higher capacity and can stand up to high speed charge/discharge than those of LIBs are demanded. Various studies have reported that the liquid phase among solid particles has a different structure from the original their properties of bulk solution (1-3). Thus solid-liquid interface is performed as a base in charge-discharge of LIBs, an elucidation of liquid phase properties of solid-liquid interface in the non-aqueous electrolyte solution system is important for improving the performance of energy storage devices such as LIBs. In addition, in late years the study of new electrolyte materials used highly-concentrated electrolytes attracts attention. Yamada et al. report that highly-concentrated

electrolytes improve charge efficiency and breakdown voltage (4). It is also very important to investigate properties of the highly-concentrated electrolytes in aiming at the performance enhancement of LIBs.

About the measurement technique, various technique such as thermodynamic measurement (2,5,6), spectrophotometric technique such as the Raman spectrometry (3,5), electrochemical measurement represented by the electric conductivity measurement (5, 7) has been used so far. We focus NMR measurement in particular(8,9). The chemical shift of NMR spectrum gives the information about structural changes and ionic processes in electrolyte solutions and it is sensitive. If molecule having high mobility due to not being restricted by ions or solids, spectrum is shape and its intensity is large because chemical exchange of nuclei is fast. On the other hand, if molecule having low mobility, spectrum is broad and its intensity is small and spectrum of molecule restricted completely is not obtained by NMR measurement. For example, results of ^{1}H static solid NMR and ^{1}H MAS NMR of water in which mesoporous silica, Si-MCM-41 and Si-SBA-15 were filled with were reported. In this report, spectra of water in water rich condition were obtained by ^{1}H static solid NMR and ^{1}H MAS NMR, but that in water poor condition was not obtain because of increase of interaction between water molecule and solid phase. In other words, water molecule which strongly interacted could not be detected by ^{1}H NMR. In addition, recent studies on molecular dynamics with NMR were carried out by spin-spin relaxation time, T_2 measurements. T_2 is defined as the process that the aligning nuclear spin after pulse irradiation returns to thermal equilibrium. In the case of ^{1}H, that process is dipolar relaxation process, so T_2 is influenced by dipole having molecule. Thus, the stronger effect of other components on solvent molecules, the shorter T_2 is. NMR is useful to obtain the knowledge of the molecular mobility.

In this study, we used non-aqueous $LiClO_4$ solution mixed with fumed silica or fumed alumina as model system of LIBs, and investigated an influence of high dispersed fumed oxide to non-aqueous electrolyte in NMR spectroscopy, effect of surface potential of solid phase and relationship between inter-molecular dynamics and intramolecular vibration by NMR and IR in order to find the interaction between solid and liquid phases in gel composite, in using the NMR spectroscopy and FT-IR measurements.

Experimental

Sample preparation

Fumed silica (200 ± 50 m$^2 \cdot$g^{-1}, FS) and fumed alumina (130 ± 50 m$^2 \cdot$g^{-1}, Alu) powder was used as solid phase, and propylene carbonate (PC) or $LiClO_4$/PC of predetermined concentration (1-3 mol/L) was used as liquid phase. Samples were prepared in Ar glovebox by complete mixing PC or $LiClO_4$/PC and FS or Alu in NMR tube. The FS and Alu powder was homogeneously dispersed in the liquid phases, respectively. A content of liquid phase were ranged from 90-100 vol% by gravimetry. Liquid content, ϕ, was determined as following equation;

$$\text{Liquid content } (\phi) = V_L / (V_L + V_S) \quad (1)$$

where V_L and V_S are the volume of liquid phase and liquid phase, respectively. In this work, the V_L and V_S values were determined from following equation;

$$V_L = W_L / \rho_L \, , \, V_S = W_S / \rho_S \qquad (2)$$

where W_L and ρ_L are the mass and the density of liquid phase, and W_S and ρ_S are those of solid phase, respectively.

^{1}H NMR measurement

The ^{1}H NMR spectra were obtained by a Varian INOVA 400 NMR spectrometer with 5mm SW probe (Varian, Inc.) To avoid mixing sample with deuterated solvent, the samples were put into inner of coaxial NMR sample tube (Wilmad-LabGlass, 516-CC-5) and D_2O was put into outer of that. The ^{1}H NMR chemical shifts were determined against external standards of deionized distilled water. The spin of the sample tubes was stopped during the measurement.

^{1}H qNMR measurement

^{1}H qNMR was performed with ^{1}H NMR spectra which was showed absolute intensity based on the principle of NMR (10). ^{1}H qNMR was defined as following equation;

$$\frac{N_x}{N_{ref}} = T \times 10^{\frac{Rg_{ref} - Rg_x}{20}} \times \frac{Ns_{ref}}{Ns_x} \times \frac{I_x}{I_{ref}} \qquad (3)$$

where N is the concentration of the chemical species that gives the NMR signal, Rg is the gain of the RF amplifier in the NMR spectrometer (i.e., receiver gain), Ns is the number of FID scans, and I is the integrated intensity of the NMR signal. The subscripts ref and x represent the external standard solution and the sample solution, respectively. T is a specific constant for the measuring system including the NMR sample tube and the entire NMR equipment, and it is almost one when a similar NMR sample tube and the same NMR equipment are used for measurements of an external standard solution and a sample solution. Because Rg and Ns can be optionally set, eq.3 shows an expression which expresses a proportion between integrated intensity of ^{1}H NMR spectra and concentration of nuclei. ^{1}H NMR measurement of deionized distilled water was performed with varying Rg and Ns in order to confirm quantitativity of eq.3.

Spin-spin relaxation time (T_2) measurement

The spin-spin relaxation time (T_2) of each sample was obtained by relaxation time measuring equipment (XiGo Nanotools, Inc., Acorn area). The sample was put into 5 mm diameter glass NMR tube. All experiments were performed at 25 ± 0.5 ˚C. We used the CPMG method showed in eq.4 (11).

$$M_{(\tau)} = M_{(0)} exp\left(\frac{-\tau}{T_2}\right) \quad (4)$$

where $M(\tau)$ is z-magnetization after pulse delay τ. In eq.4, T_2 value that averaged all intramolecular nuclear relaxation is obtained in this method.

FT-IR spectroscopy measurement

IR spectrum was measured by Fourier transform-infrared spectrometer (FT-IR; JASCO Co., FT/IR-615R). The measurement was performed by diffuse reflection method (JASCO Co., DR-400) The conditions were as follow; 4 cm^{-1} resolution, 256 scan, MCT detector.

Results and Discussion

^{1}H NMR measurement

The $LiClO_4$ concentration dependences of ^{1}H NMR without solid phase were shown in Fig. 1. The peak of each signal shifts to the low magnetic field by changing of the physical property of solvent according to the increase of $LiClO_4$ concentration. The widths of each signal remarkably broaden in the salt concentration of more than 3 mol/L. This shows the destruction of the network structure of the solvent by the increase of the salt concentration. The result of ^{1}H NMR spectroscopy measurement of pure PC/FS samples indicated in Fig. 2. A broad signal was confirmed under the existence solid-phase. It was shown that the dynamic property of PC molecules largely decreased in comparison with the case only for liquid phases. ^{1}H NMR spectra shifted to higher magnetic field with the decrease of liquid content. For the shielding effect to the ^{1}H nucleus of the PC

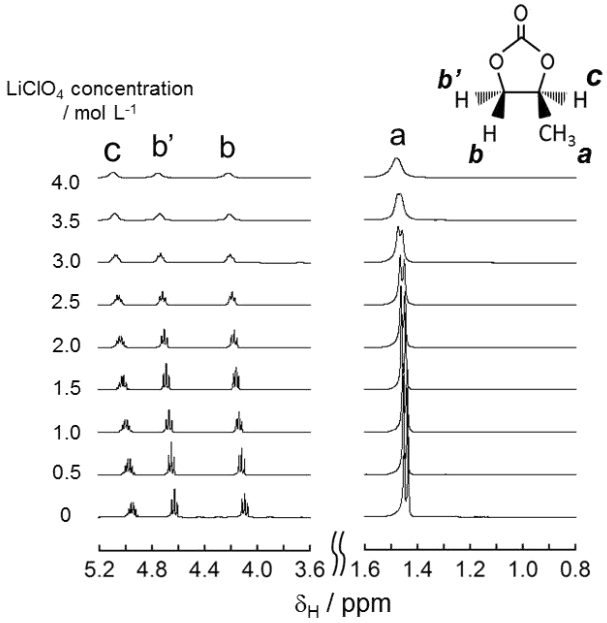

Fig. 1 $LiClO_4$ concentration dependences of ^{1}H NMR without solid phase of propylene carbonate solution of $LiClO_4$.

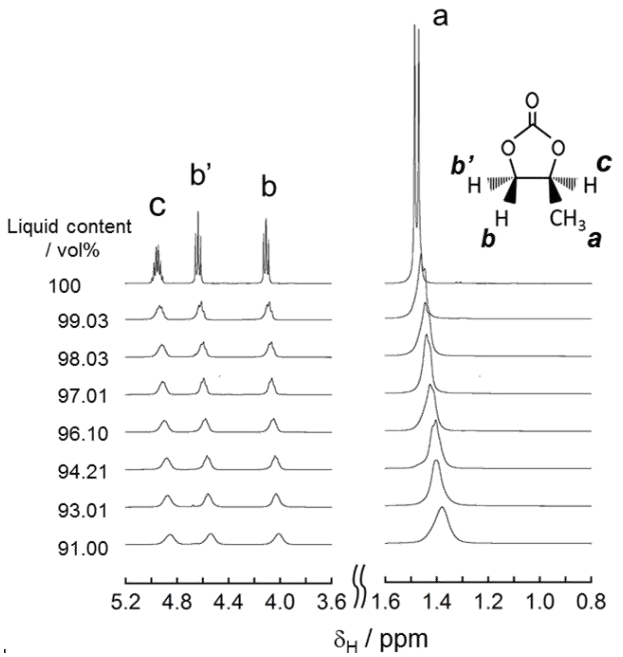

Fig. 2 Liquid content dependence of the ^{1}H NMR spectra for fumed silica powder + propylene carbonate systems. The measurement samples does not contain any electrolyte.

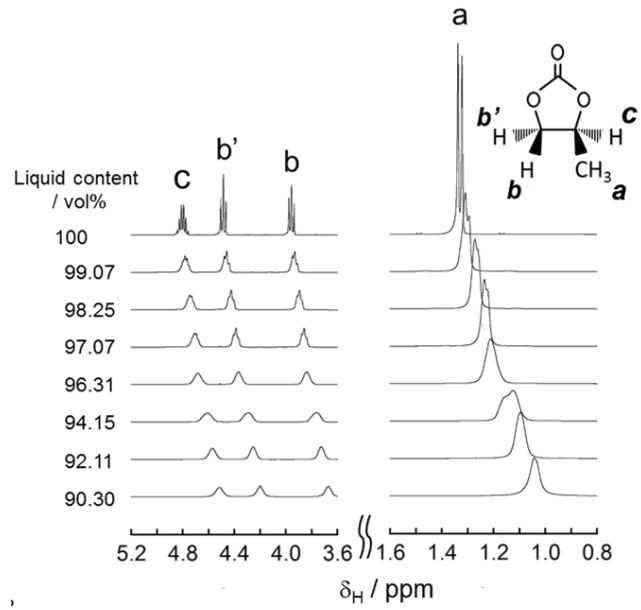

Fig. 3 Liquid content dependence of the ^{1}H NMR spectra for fumed alumina powder + propylene carbonate systems. The measurement samples does not contain any electrolyte.

molecules by the surface negative charge of fumed silica surface, a signal continues to shift to higher magnetic field as a content of solid-phase increases. This result suggested that the apparent charge densities around the proton of PC molecules increased by fumed silica because fumed silica surface has a negative charge.

The result of ^{1}H NMR spectroscopy measurement of pure PC/Alu samples indicated in Fig. 3. In the fumed alumina system, ^{1}H NMR signal continues to shift to higher

magnetic field with the decrease of liquid content. This higher magnetic field shift was remarkable than the case of PC/FS system. Then, plots of chemical shift of each peak were illustrated in Fig. 4. In alumina dispersion, NMR signal shifted to higher magnetic field than that of fumed silica surface. From this result, alumina gives more influence on dynamics properties of liquid phase. A similar result was observed in 1-3 mol/L $LiClO_4$/PC and solid coexisting system.

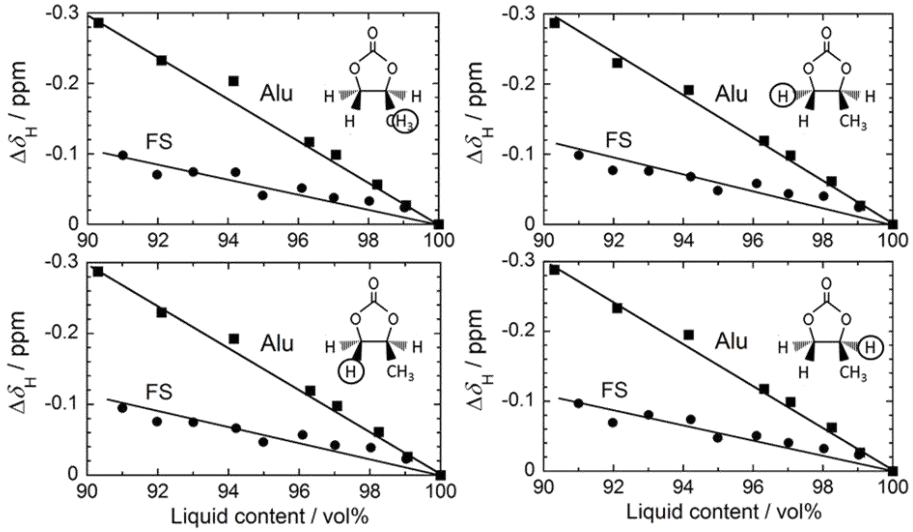

Fig. 4 Dependences of the ^{1}H NMR chemical shift changes on the liquid content for fumed silica powder + propylene carbonate and fumed alumina powder + propylene carbonate systems. The measurement samples does not contain any electrolyte.

^{1}H qNMR measurement

The liquid content dependences of the ^{1}H NMR detection ratios of propylene carbonate were shown in Fig. 5. The ^{1}H NMR detection ratios are determined by the ratio of the overall signal intensity due to propylene carbonate for the sample without solid phase and that for the sample with solid phase. Peak intensity is the sum total of each proton and the dashed line in each figure represented the theoretical value of detected amount of PC by ^{1}H NMR. From Fig. 5, almost same amount of PC molecules was detected in PC/FS coexisting system. This result indicated that fumed silica formed network structure but H of PC molecules remained its dynamics. On the other hand, in fumed alumina dispersion, values of PC molecules detected by NMR decreased compared to dashed line. It suggests that the mobility of PC molecules in fumed silica system were restricted than that in alumina system.

^{1}H Spin-spin relaxation time (T_2) measurement

Results of ^{1}H spin-spin relaxation time (T_2) in bulk solution system is shown in Fig. 6. From Fig. 6, as Li^+ ion concentration increases, T_2 decreased remarkably. It relates the change of viscosity. The relaxation time by dipole-dipole interaction, i.e., T_{1DD} and T_{2DD}, is expressed by using correlation time as following equations (12);

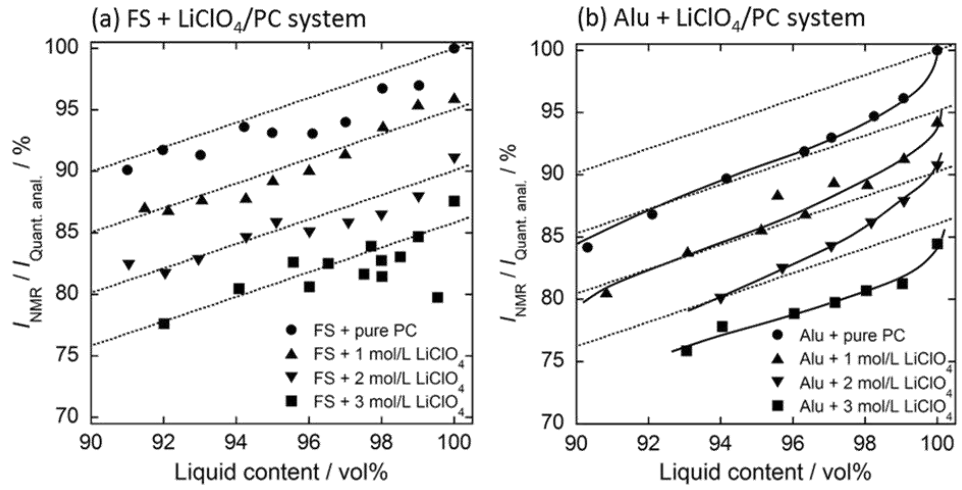

Fig. 5 Liquid content dependence of the ^{1}H NMR detection ratios of propylene carbonate. The ^{1}H NMR detection ratios are determined by the ratio of the overall signal intensity due to propylene carbonate for the sample without solid phase and that for the sample with solid phase. (a) fumed silica powder + x mol/L $LiClO_4$ propylene carbonate solution systems (x=0-3). (b) fumed alumina powder + x mol/L $LiClO_4$ propylene carbonate solution systems (x=0-3).

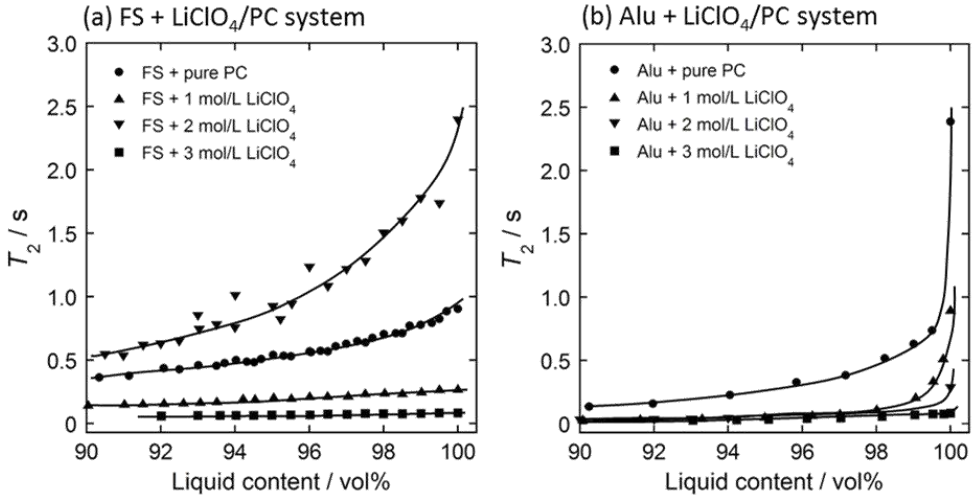

Fig. 6 Liquid content dependence of the spin-spin relaxation time, T_2, of ^{1}H NMR due to propylene carbonate. The measurement samples are as described in the caption of Fig. 5.

$$\tau_c = \frac{4\pi a^3}{3k} \cdot \frac{\eta}{T} \tag{5}$$

$$\frac{1}{T_{1DD}} = \frac{1}{T_{2DD}} = 10a \frac{\gamma^4}{r^6} \tau_c \tag{6}$$

where η is the viscosity, T is the temperature, and a is the radius of the molecule of the

sample liquid, respectively, and k is the Boltzmann constant. From eqs.5 and 6, as viscosity increases, the relaxation time shortens. Because only PC molecules of only 11 mol exist for Li^+ ion of 1 mol per 1 L in the PC system for it, most PC molecules solvate with Li^+ ion. Therefore, the structure of the whole solvent is greatly affected by the addition of the Li^+ ion, and relaxation time largely decreased. This result is supported from a rise of the viscosity with the increase of concentration of $LiClO_4$/PC solution.

T_2 in solid-liquid coexisting system is also shown in Fig. 6. From Figs. 6(a) and 6(b), in both systems, i.e., FS + LiClO4/PC and Alu + LiClO4/PC systems, the T_2 value decreases because the dynamics of water molecules of the liquid phase decrease in solid-liquid coexisting system. The T_2 value greatly fell down in the fumed alumina system in comparison with fumed silica system. The influence of the solid surface to solvent mobility in fumed silica dispersion is much less than that in fumed alumina dispersion. This result supports a signal of the NMR and the result of ^{1}H qNMR measurement.

FT-IR spectroscopy measurement

The result of FT-IR spectroscopy measurement of each system indicated in Fig. 7. FT-IR spectroscopy is an analytical method which detects the change of dipole moment associated with molecular vibration. In the case of the method is applied for solid-liquid coexisting system, the change of vibration mode by solid particle is detected. In pure solvent system, the single peak of C=O stretching vibration of PC was observed in 1780 cm^{-1}. In solid-liquid coexisting system, this peak mainly separated two peaks. Lower wavenumber peak is based on a direct interaction between solid phase and O=C bonding, and higher wavenumber peak is based on free C=O stretching vibration. In alumina system, the higher wavenumber peak was observed more than the lower one. This result indicated indirect electron-donation from solid surface which are corresponding of shift to higher magnetic field in ^{1}H NMR signal.

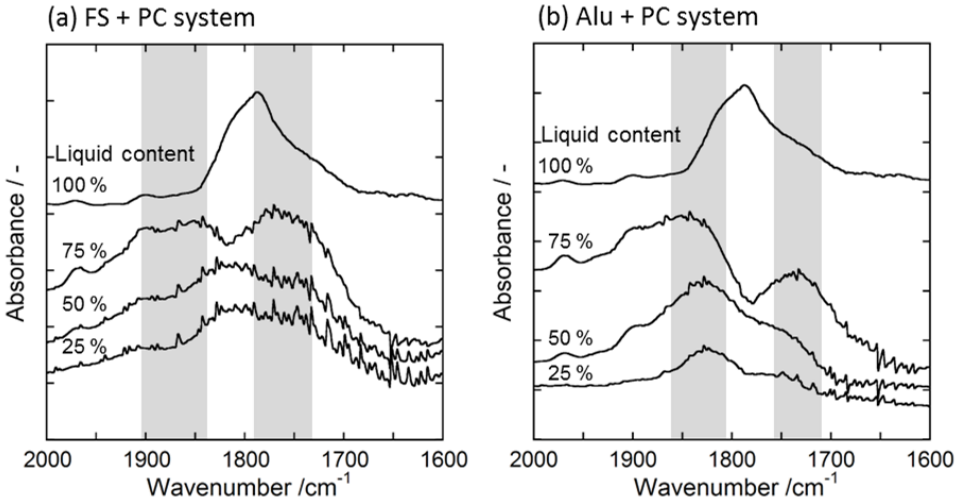

Fig. 7 FT-IR spectra of C=O stretching vibration of propylene carbonate. (a) fumed silica powder + propylene carbonate. The measurement samples does not contain any electrolyte. (b) fumed alumina powder + propylene carbonate.

Conclusion

NMR signal of ^{1}H in PC molecules is influenced by coexisting solid phase in $LiClO_4$-PC solution /oxide powder. The variation of NMR signal depends on surface acidities of oxide. In IR spectra of PC/Alumina systems, the vibration in higher wavenumber range are predominantly observed due to indirect electron-donation from solid surface. The signal intensity depends on influenced liquid content from solid phase. Especially, the $LiClO_4$-PC solution /alumina systems, the intensity is abruptly decreased due to widely spread influences of solid phases. The dissolution state and the physical properties, in particular the molecular mobility, of the PC solvent and the electrolyte in the solid-liquid interface, obtained in this study are useful for the achievement of a highly effective ion transport in a practical secondary battery. The clarification of the ion transport in densified micro-, meso-, and macroporous in porous electrode which is represented by the electrode of LIBs will give the design guidelines of the acceleration of Li^+ ion movement (insertion-desertion reaction) reaction between complicated electrode/electrolyte heterointerfaces in a composite electrode where the active material, the conductive assistant, and the binder exist together.

This study was supported by the JST Core Research for Evolutional Science and Technology (CREST).

References

1. M. Mizuhata, H. Ikeda, A. Kajinami, and S. Deki, *J. Mol. Liq.*, **83**, 179-189 (1999).
2. S. Deki, A. Kajinami, Y. Kanaji, M. Mizuhata, and K. Nagata, *J. Chem. Soc. Faraday Trans.*, **89**, 3811-3815, (1993).
3. A. B. Béléké, M. Mizuhata, and S. Deki, *Vib. Spectrosc.*, **40**, 66-79, (2006)
4. Y. Yamada, K. Furukawa, K. Sodeyama, K. Kikuchi, M. Yaegashi, Y. Tateyama, and A. Yamada*, J. Am. Chem. Soc.,* **136**, 5039-5046, (2014).
5. M. Mizuhata, Y. Sumihiro, and S. Deki, *Phys. Chem. Chem. Phys.,* **6,** 1944-1951, (2004).
6. M. R. Landry, *Thermochim. acta,* **433**, 27-50, (2005)
7. S. Deki, S. Nakamura, A. Kajinami, Y. Kanaji, and M. Mizuhata, *J. Chem. Soc. Faraday Trans.*, **89**, 3805-3810, (1993).
8. P. Porion, A. M. Faugère, and A. Delville, *J. Phys. Chem. C,* **118**, 20429-20444, (2014).
9. B. Grünberg, T. Emmler, E. Gedat, I. Shenderovich, G. H. Findenegg, H.-H. Limbach, and G. Buntkowsky, *Chem. Eur. J.*, **10**, 5689-5696, (2004).
10. H. Maki, Y. Okumura, H. Ikuta, and M. Mizuhata, *J. Phys. Chem. C*, **118**, 11964-11974 (2014).
11. S. Meiboom, and D. Gill, *Rev. Sci. Instrum.*, **29**, 688-691 (1958).
12. J. W. Akitt, in *NMR and Chemistry: An Introduction to Modern NMR Spectroscopy*, Chap. 4.2, Chapman & Hall, London, 3rd edn, 1992.